American Mineralogist, Volume 74, pages 1325–1336, 1989

Stacking variations and nonstoichiometry in the bixbyite-braunite polysomatic mineral group

JOHAN P. DE VILLIERS,* PETER R. BUSECK
Departments of Geology and Chemistry, Arizona State University, Tempe, Arizona 85287, U.S.A.

ABSTRACT

Bixbyite, braunite, neltnerite, and braunite-II are members of a mineral group based on the cation arrangement of the fluorite structure type, with general formula M_8O_{12} (M = Mn, Fe, Ca, Si). They consist of layer modules of (Mn,Fe)-O octahedra stacked in various sequences that depend on the coordination of interlayered M cations.

The structures of 21 possible layer assemblages have been generated using stacking vectors derived from the known mineral varieties. These structures have been used to simulate the images obtained by electron microscopy.

Nonstoichiometry has been observed in braunites from several localities and is manifested by variations in their M^{2+} and Si contents. High-resolution transmission electron microscopy (HRTEM) revealed the presence of several layer assemblages of different thicknesses. In addition to the 2-module bixbyite, the 4-module braunite, and the 8-module braunite-II, new 3-, 5-, and 8-module assemblages have been observed. These assemblages have calculated SiO_2 contents that vary between 0 and 10 wt%.

Fine intergrowths of bixbyite (free of silica) and braunite-II (5 wt% SiO_2) have also been observed by HRTEM. These intergrowths consist of different amounts and thicknesses of the two components and account for nonstoichiometric variations in the M^{2+} and Si contents lower than those for braunite-II.

INTRODUCTION

There is a close relationship between the crystal chemistry and mechanism of silica substitution among bixbyite (Mn_2O_3), braunite ($Mn^{2+}Mn_6^{3+}SiO_{12}$), braunite-II ($Ca_{0.5}Mn_7^{3+}Si_{0.5}O_{12}$), and neltnerite ($CaMn_6^{3+}SiO_{12}$). They can be described by the general formula M_8O_{12} and also can be considered members of a polysomatic series, as defined by Thompson (1978). There is a considerable range of composition among these minerals, and their structural relations are complex.

The bixbyite-braunite minerals are related by stacking variations of three polyhedral layers (Moore and Araki, 1976). Alternatively, these structures can be generated by stacking a unique polyhedral layer using different stacking vectors and by placing cations in cubic, octahedral, or tetrahedral sites between the polyhedral layers. Crystal data for the various ordered members are given in Table 1.

The study by Geller (1971) provided the basis for the comparison of the structures of bixbyite and braunite by Moore and Araki (1976). Geller also determined that pure Mn_2O_3 (partridgeite) is orthorhombic (pseudocubic), as compared to the cubic structure of bixbyite, which contains >0.75 mol% Fe. Neltnerite was described by Baudracco-Gritti et al. (1982) as the Ca analogue of braunite. It had previously been shown by Damon et al. (1966) that this mineral, subsequently named neltnerite, is isostructural with braunite.

Electron-microprobe analyses by Baudracco-Gritti (1985) and Kleyenstüber (1985) provided much-needed chemical data for members of this group. Those studies showed that many braunites are not stoichiometric in their M^{2+} and Si contents. In the present study, single-crystal X-ray diffraction investigations of the nonstoichiometric varieties were inconclusive because many of the weak superstructure reflections were masked by streaking parallel to c^*, produced by stacking disorder.

The bixbyite-braunite minerals provide an interesting example of polysomatism. They consist of modules (layers) of different compositions, stacked in various proportions and with different stacking vectors. Other terms that have been used for minerals related by polysomatism are "mixed-layer polytypism" (Kohn and Eckart, 1965) and "homologous series" (Magneli, 1953). In this paper we use the nomenclature of Thompson (1978) and refer to a crystal consisting of chemically distinct layer modules as being a polysome. Additionally, in order to describe the single or multiple layers having stacking sequences different from those of the host crystal, we use the term "layer assemblage" or simply "assemblage." Where such assemblages occur as ordered crystals, they form polysomes.

The goal of the present study was to determine the stacking sequences in ordered and disordered members

* Present address: Mineralogy Division, Mintek Private Bag X3015, Randburg, 2125, South Africa.

0003–004X/89/1112–1325$02.00

TABLE 1. The bixbyite-braunite group

Mineral	Formula	Space group	Cell parameters Å	Reference
Partridgeite	Mn_6O_{12}	*Pcab*	$a = 9.42$ $b = 9.42$ $c = 9.40$	Geller, 1971
Bixbyite	$(Mn,Fe)_8O_{12}$	*Ia*3	$a = 9.41$	Geller, 1971
Braunite	$Mn^{2+}Mn^{3+}_6SiO_{12}$	$I4_1/acd$	$a = 9.42$ $c = 18.70$	de Villiers, 1975
Neltnerite	$CaMn^{3+}_6SiO_{12}$	$I4_1/acd$	$a = 9.46$ $c = 18.85$	Baudracco-Gritti et al., 1982
Braunite-II	$Ca_{0.5}Mn^{3+}_7Si_{0.5}O_{12}$	$I4_1/acd$	$a = 9.43$ $c = 37.77$	de Villiers, 1980

of the bixbyite-braunite group through the use of high-resolution transmission electron microscopy (HRTEM) and analytical electron microscopy (AEM). These observations were then used to interpret the mineral stoichiometries.

EXPERIMENTAL METHODS

Single crystals of members of the bixbyite-braunite group were selected for analysis. They are bixbyite (from Lohatla, Postmasburg, South Africa), braunite-II (Tachgagalt, Morocco, and Middelplaats mine, Hotazel, South Africa), and disordered braunite (Dibiaghomo, Hotazel, South Africa). A precession camera was used to orient these crystals to have their [100] zone axes parallel to the X-ray beam. The crystals were then glued onto a glass slide that was oriented parallel to the layer-line screen. The crystals were ground to a thickness of approximately

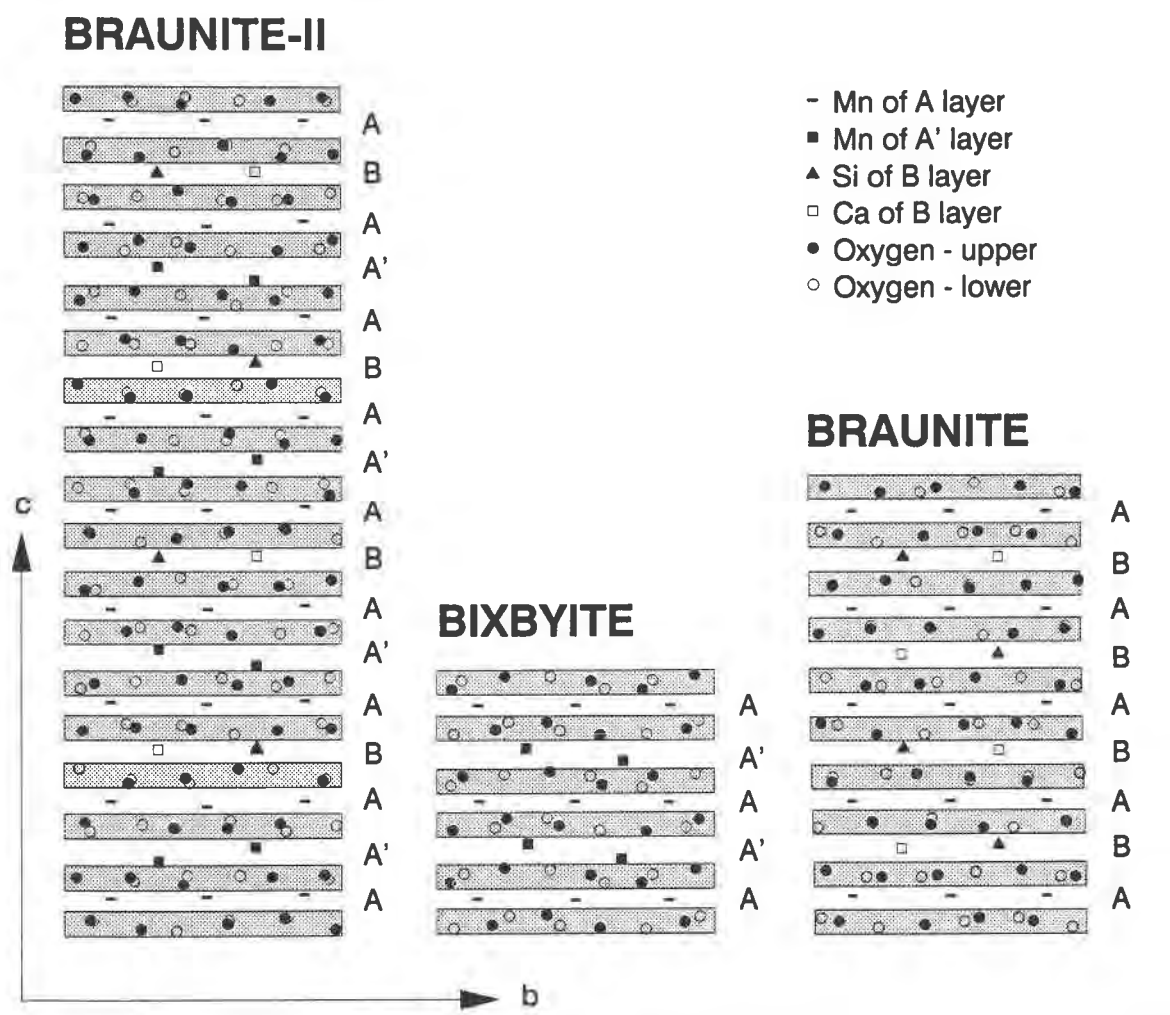

Fig. 1. Sections (at height $x \approx 0$) through the structures of braunite-II, bixbyite, and braunite showing the stacking sequence of the A, A', and B cation layers. "Oxygen—upper" and "oxygen—lower" denote oxygen atoms above and below x, respectively.

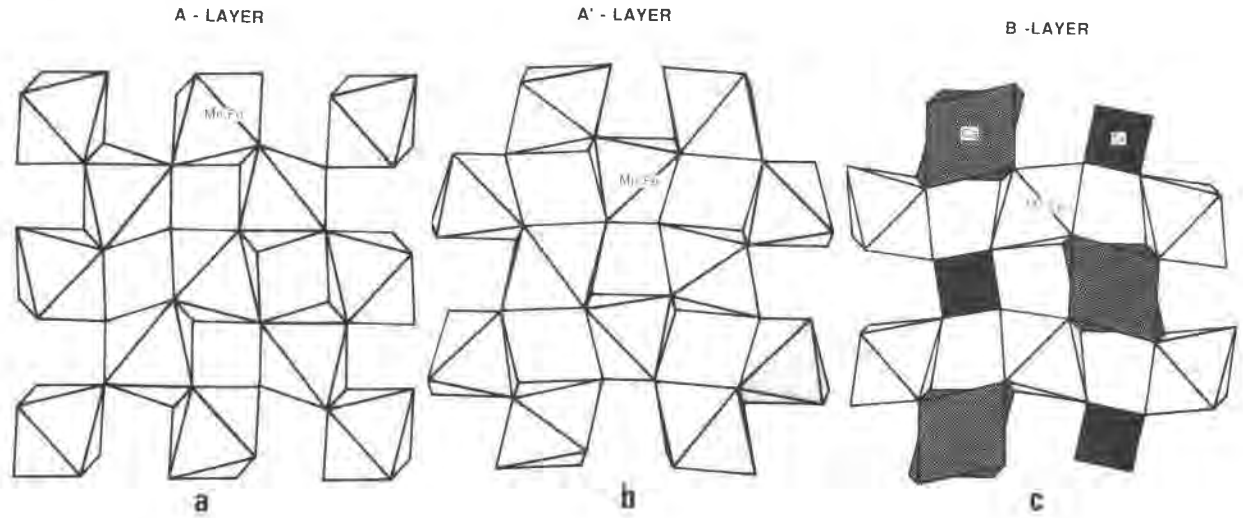

Fig. 2. (a) The A-layer module common to all bixbyite-braunite polysomes. (b) The A′-layer module, which is present in bixbyite and braunite-II. (c) The B-layer module, which occurs in braunite and braunite-II. All three diagrams are *c*-axis projections.

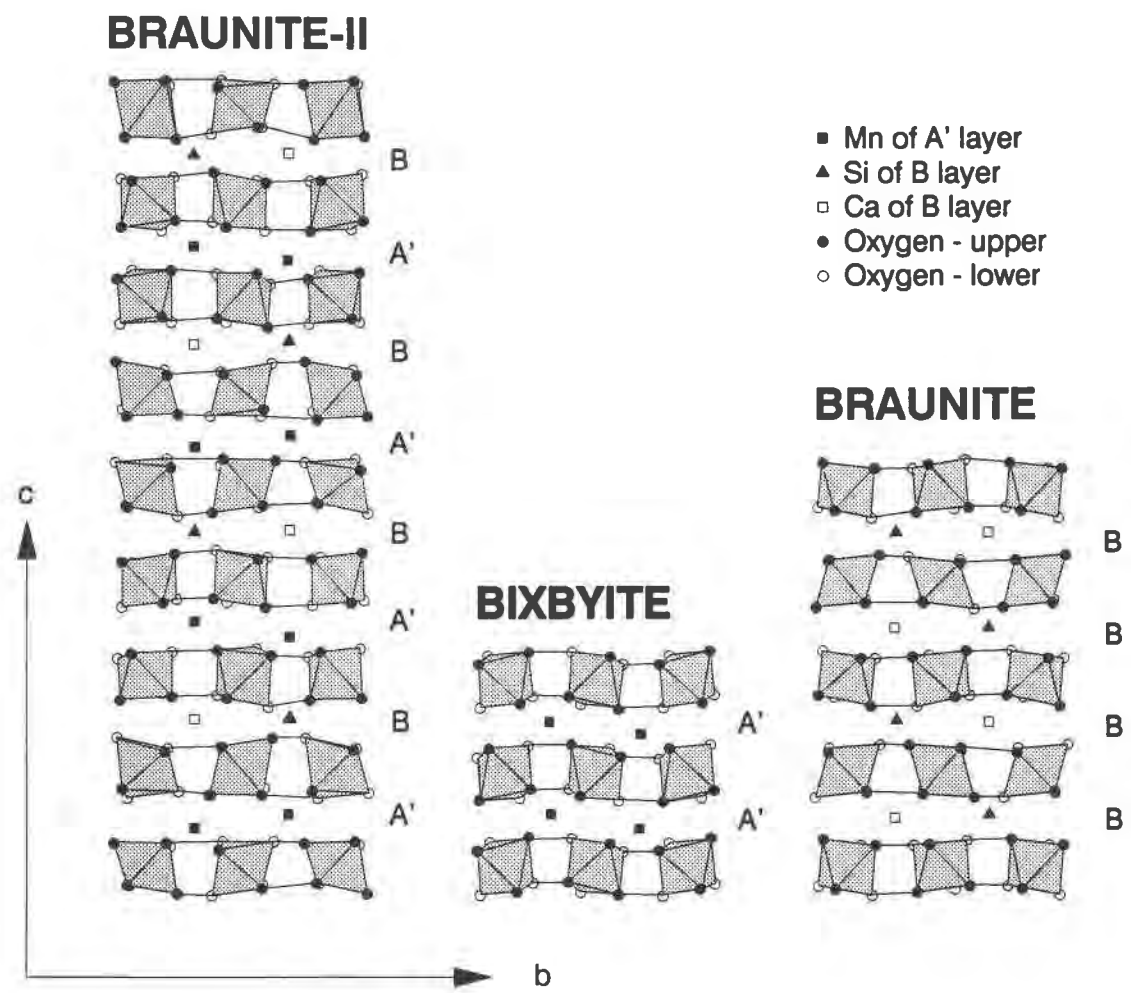

Fig. 3. Sections (at height $x \approx 0$) through the structures of braunite-II, bixbyite, and braunite showing the sequence of cation layers situated between A-layer modules containing Mn-O octahedra. This figure is drawn to the same scale as Fig. 1.

30 μm and analyzed with a JEOL JXA 8600 electron microprobe, operated at 15 kV with a sample current of 10 nA. Wollastonite (Ca,Si), MnO (Mn), and hematite (Fe) were used as standards. The Tracor Northern TASK program containing standard ZAF matrix corrections was used to acquire and correct the raw intensity data. The same crystals were then mounted over pinholes in Mo-foil sample holders and ion-milled for transmission electron microscopy. This procedure ensured proper crystal alignment with respect to the electron beam. Single crystals as small as 50 μm were oriented and thinned in this fashion.

The samples were initially examined using a JEOL 200CX electron microscope operated at 200 keV with an LaB_6 filament and equipped with a ±12° double-tilt, top-entry goniometer stage. The spherical aberration coefficient, C_s, of the objective lens was 1.2 mm, and a 400-μm condenser aperture was used, together with various sizes of objective apertures for bright-field and multi-beam HRTEM modes. Beam damage in these materials was negligible, and magnifications of 270000 to 530000 were used to record the HRTEM images.

Most samples were also examined in a JEOL 4000EX microscope operated at 400 keV, equipped with a ±15° double-tilt, top-entry goniometer stage. C_s was 1.0 mm, and condenser and objective apertures of 150 μm and 40 μm were used, respectively.

Selected regions of the samples were subsequently examined in a Philips 400T analytical electron microscope operated at 120 keV. The energy-dispersive spectra were obtained with beam sizes of approximately 400 Å using a Tracor Northern TN2000 analyzer. Compositions were calculated using predetermined k factors and the ANEDS programs, developed at Arizona State University. The stoichiometry was calculated assuming the presence of Mn^{3+} and Fe^{3+} in the crystals.

Image simulations

Image simulations of the ordered structures were performed with the Ishizuka multislice program (Ishizuka and Uyeda, 1977), using atomic parameters from de Villiers (1975, 1980) and Geller (1971). The atomic parameters of the other polysomes were generated by a specially written computer program (CAT-POS) using a stacking algorithm, and these positions were used as input for the image-simulation program. In all cases, structure factors were calculated for atom positions over the full unit cell. Slice thicknesses of 1.6 Å as well as beam divergences of 0.0001 and 0.0008 radians were used to simulate the 200CX and 4000EX microscope images. All calculations were done for the a-axis projections.

Structures

Members of the bixbyite-braunite group have fluorite-related structures and can be described in terms of three layer modules, the A, A′, and B layers (Moore and Araki, 1976). As can be seen from Figure 1, which is a section (at approximately $x = 0$) through the structures, the A-, A′-, and B-cation layers are separated by layers of oxygen atoms. These oxygens are shared by adjacent cation layers. If coordination polyhedra are constructed around all the A, A′, and B cations, the layer modules shown in Figures 2a, 2b, and 2c are produced. The sharing of oxygens means that adjacent polyhedra are linked above, below, and within the plane of projection. Adjacent layer modules thus share oxygen atoms. These polyhedral layer modules form the basis of the structural description by Moore and Araki.

The A-layer module consists of Mn-O octahedra and occurs in all observed and postulated structures. The A′-layer module also consists of Mn-O octahedra (these are more distorted than in the A layer), and it is present in bixbyite and braunite-II. The B-layer module consists of M^{2+} (usually Mn^{2+} or Ca) in distorted cubic coordination, Si in tetrahedral coordination, and Mn^{3+} in octahedral coordination. Since these B-layer octahedra are located at $x \neq 0$, the B-layer Mn atoms do not appear in Figure 1. This B layer occurs in braunite, braunite-II, and neltnerite. Where Ca is present, the cubic coordination polyhedron is less distorted than where Mn^{2+} occurs (de Villiers, 1980). The stacking sequence of the layer modules in bixbyite is $[AA']_2$, in braunite and neltnerite it is $[AB]_4$, and in braunite-II it is $[AA'AB]_4$ (Fig. 1).

The structures can also be described in terms of variations in the stacking of the A-layer modules. The atom positions in Figure 3 are identical to those in Figure 1, but polyhedra are constructed around only the cations in the A layers. The effect is that the structures can now be described in terms of the cations located between the A layers. To conform to the Moore and Araki (1976) nomenclature, cations that occur in the A′ or B layer modules are called A′ and B cations. Thus, bixbyite, which is described as $[AA']_2$ in the Moore and Araki formalism, now becomes $[A']_2$, braunite and neltnerite go from $[AB]_4$ to $[B]_4$, and braunite-II goes from $[AA'AB]_4$ to $[A'B]_4$. In this alternative description, the A-layer symbols are omitted.

In order to match the observed and simulated electron-microscope images, it was necessary to generate the atomic positions for all possible polysomes. This was done in two steps. A computer program (BUILD-LAYERS) was written to check every stacked A layer for coincidence with the initial A layer module and thereby determine all possible stacking sequences for up to eight modules. The test was performed after each successive stacking operation. The identities of the stacking vectors depend on the sequence of interstitial cations and are given in Table 2. A total of 2^8 possible stacking sequences were tested for

Table 2. A-layer stacking vectors

Operation*	Stacking vectors**
A′–B–A′	¼ − y, ¼ − x, 2 − Z
B–A′–B	½ − x, ½ − y, 4 − Z
A′–A′–A′	½ + x, ½ + y, 1 + Z
B–B–B	¼ + y, ¼ + x, 1 + Z

* Only the interstitial cation stacking sequence is shown. The A layers are situated between the designated cations.

** The Z coordinate is that of a single A-layer module, i.e., $Z = 8 \cdot z$ for braunite-II, $4 \cdot z$ for braunite, and $2 \cdot z$ for bixbyite.

TABLE 3. Polysomes of the bixbyite-braunite group (for up to 8 A-layer modules)

Assemblage	Sequence	Thickness (Å)	SiO_2 (wt%)
Known polysomes			
1. Bixbyite (2-module)	A′A′	9.4	0.0
2. Braunite (4-module)	BBBB	18.8	10.0
3. Braunite-II (8-module)	BA′BA′BA′BA′	37.8	5.0
Calculated polysomes			
4. (3-module)	BA′B	14.2	6.7
5. (6-module)	BBBA′BA′	28.3	6.7
6. (7-module)	BA′A′BA′A′A′	33.1	2.8
7. (8-module)	BBBA′A′BA′A′	37.8	5.0
8. (8-module)	BBBA′A′A′BA′	37.8	5.0
Calculated mixed-module* polysomes			
9. (5-module) (4) + (1)	BA′BA′A′	23.6	4.0
10. (5-module) (4) + (1)	BBA′A′A′	23.6	4.0
11. (6-module) (2) + (1)	BBBBA′A′	28.3	6.7
12. (7-module) (2) + (4)	BBBBBBA′	33.1	8.6
13. (7-module) (4) + 2(1)	BBA′A′A′A′A′	33.1	2.9
14. (7-module) (4) + 2(1)	BA′BA′A′A′A′	33.1	2.9
15. (8-module) (2) + 2(1)	BBBBA′A′A′A′	37.8	5.0
16. (8-module) (6) + (1)	BBBA′BA′A′A′	37.8	5.0
17. (8-module) 2(4) + (1)	BBA′BBA′A′A′	37.8	5.0
18. (8-module) (4) + (9)	BBA′BA′BA′A′	37.8	5.0
19. (8-module) (4) + (9)	BBA′BA′A′BA′	37.8	5.0
20. (8-module) (4) + (4) + (1)	BBA′A′BBA′A′	37.8	5.0
21. (8-module) (4) + (9)	BBA′A′BA′BA′	37.8	5.0

* The mixed-module polysomes consist of a regular interlayering of the indicated polysomes listed as numbers 1 to 5. For example, polysome no. 9, [BA′BA′A′], can be viewed as a 1:1 mixture of polysomes no. 4, [BA′B], and no. 1, [A′A′]. Polysome no. 10, [BBA′A′A′], can also be viewed as a mixture of polysome no. 4, [BBA′] (which is equivalent to [BA′B]), and polysome no. 1, [A′A′].

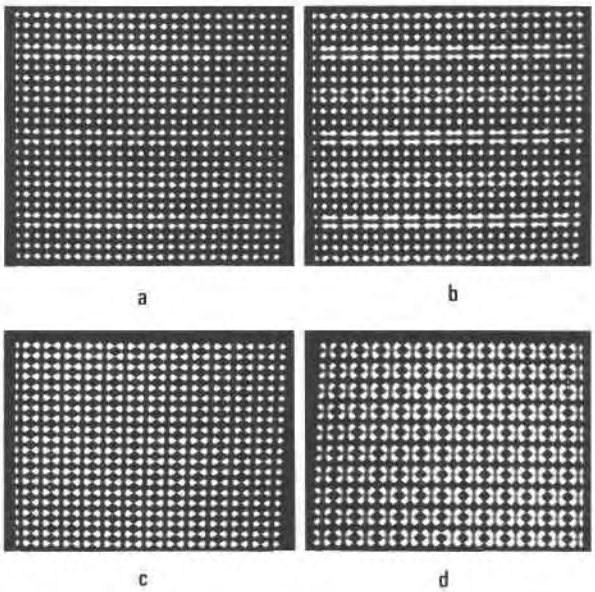

Fig. 4. (**a** and **b**) Calculated images of braunite-II and (**c** and **d**) bixbyite. Images a and c were calculated from atomic coordinates derived from an X-ray structure analysis, whereas images b and d were calculated from atomic coordinates derived from the program generating different polysomes.

coincidence. Twenty-one distinct polysomes resulted (Table 3). In the next step, the A-layer atomic positions were generated by the program CAT-POS, and the A′ or B cations were placed in the interlayer octahedral, cubic, or tetrahedral sites generated by the postulated stacking operation.[1]

The atomic positions of braunite-II were taken as the basis for generating the other structures from interstitial cation and common A-layer atom positions. The braunite-II structure contains both A′ and B cations, whereas bixbyite contains only A′ and braunite only B cations (Fig. 3). Furthermore, displacement vectors of $(\frac{1}{4} + y)$, $(\frac{1}{4} - x)$, $(\frac{1}{16} + z/4)$ and $(\frac{1}{4} + y)$, $(\frac{3}{4} - x)$, $(\frac{1}{16} + z/2)$ were used to bring the initial A-layers and interstitial cations of bixbyite and braunite, respectively, into correspondence with those of braunite-II.

Using the computed coordinates, the calculated images of braunite-II and bixbyite were compared to those calculated by use of the atomic coordinates obtained from single-crystal X-ray structure analysis (Fig. 4). Except for minor differences in contrast, these images match closely. The atomic coordinates of the two sets also agree closely, with the minor variations mainly in the cation positions. The simulated images of the polysomes listed in Table 3 can thus be readily calculated in order to match the observed HRTEM images with the postulated polysomes.

MINERAL CHEMISTRY

Electron-microprobe analyses by Baudracco-Gritti (1985) of samples of braunite and braunite-II show a remarkable spread in composition, ranging continuously from those of braunite to braunite-II. Variations in SiO_2 contents within single crystals were observed. There is also evidence of Ca substitution in the analyzed braunites. The neltnerite compositions, on the other hand, are constant and correspond closely to the stoichiometric composition.

The compositions of disordered braunites from the Kalahari manganese field, determined by Kleyenstüber (1985) and by ourselves, are shown in Figure 5. The two sets of analyses are compatible. Our analyses were performed on selected, optically homogeneous, single crystals with a predominant tetragonal bipyramidal habit. The mineral compositions clearly show extensive variability in their SiO_2 contents, ranging from pure bixbyite toward the neltnerite composition. This variation cannot be explained in terms of a simple solid-solution model, since the substitution involves small Si and large Ca atoms for Mn atoms. Different valencies of the substituting cations and the Mn cations also make substitution on specific sites, without changing the oxygen coordination around these cations, unlikely. The compositions of the bixbyite, braunite-II, and disordered braunite that were selected for HRTEM study are given in Table 4.

[1] A list of the postulated cation coordinates may be ordered as Document AM-89-423 from the Business Office, Mineralogical Society of America, 1625 I Street, N.W., Suite 414, Washington, D.C. 20006, U.S.A. Please remit $5.00 in advance for the microfiche.

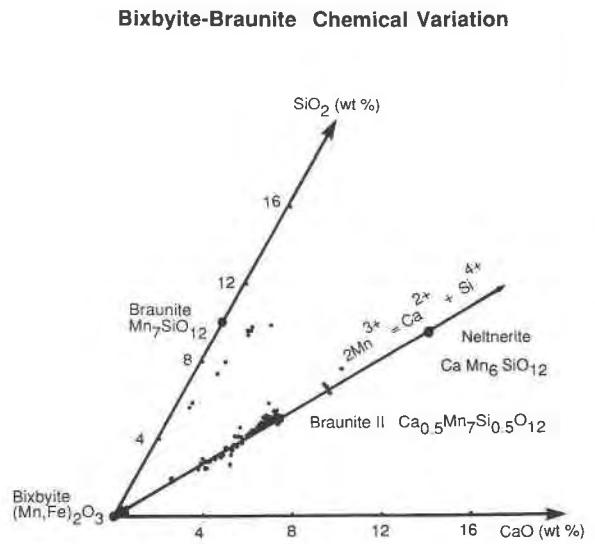

TABLE 4. Compositions of crystals used for HRTEM study

	(a)	(b)	(c)	(d)	(e)	(f)
CaO	n.d.	n.d.	4.87	4.76	3.92	4.68
MgO	0.07	0.07	0.03	0.01	n.d.	0.02
SiO_2	0.04	0.00	5.01	5.01	4.05	4.67
Al_2O_3	2.08	2.02	0.08	0.11	0.30	0.26
Fe_2O_3	13.91	14.86	11.10	12.44	10.31	8.91
Mn_2O_3	84.90	82.56	79.74	76.95	80.52	81.87
Total	101.00	99.51	100.83	99.28	99.10	100.41

Note: (a), (b) Bixbyite single crystal from Postmasburg. (c) Braunite-II from Tachgagalt, Morocco. (d) Braunite-II from Middelplaats mine, Hotazel. (e), (f) Disordered braunite from Dibiaghomo, Hotazel. n.d. = not detected.

←

Fig. 5. Compositional variation of bixbyite-braunite minerals from the Kalahari manganese field plotted on an SiO_2-$(Mn,Fe)_2O_3$-CaO ternary diagram. Most braunites lie on the line representing the exchange of a Ca and a Si atom for two Mn atoms.

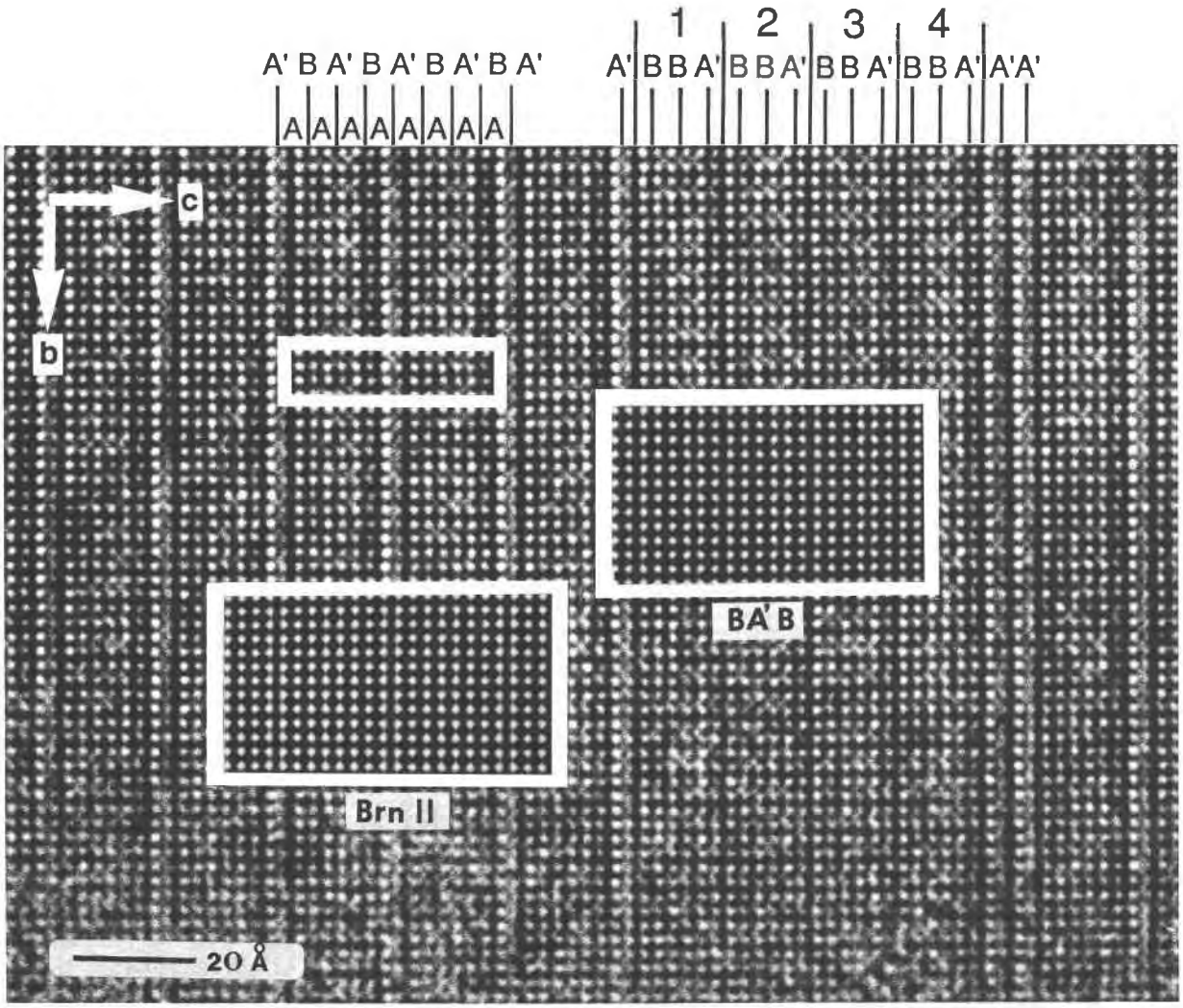

Fig. 6. A layer consisting of four repeat units of the 14.2-Å [BA'B] layer assemblage in disordered braunite from the Dibiaghomo locality. The regular 37.8-Å braunite-II unit cell is also indicated, as are the calculated images of the two polysomes.

ELECTRON MICROSCOPY OF LAYER ASSEMBLAGES

As mentioned above, structural units that we call layer assemblages, or simply assemblages, can occur within otherwise ordered host crystals. Such assemblages have the individual structural elements of polysomes and are commonly observed by HRTEM. Since they do not necessarily repeat themselves enough to be periodic (see, for example, the discussions by Veblen and Buseck, 1979, and Buseck and Veblen, 1988), they are not true polysomes, although they would form polysomes if the units repeated enough to be periodic.

The electron-microscope investigation of braunite-II single crystals revealed the existence of several different layer assemblages, even in very well ordered materials. Such assemblages are evident in the electron-microscope images as layers of different thicknesses and contrast.

Aside from bixbyite, the polysome with the smallest repeat unit, 14.2 Å, is postulated to be the 3-module [BA′B] sequence, shown as number 4 in Table 3. As an assemblage, it is present in disordered braunite and is shown in Figure 6 occurring as four repeat units in a 60-Å-thick layer. Three repeat units, calculated from the postulated atomic coordinates, are superimposed on the HRTEM image. The match between experimental and calculated images confirms our interpretation. The SiO_2 content of this assemblage is 6.7 wt%. The unit cell of braunite-II is outlined and consists of two 18.8-Å layers as a result of I-centering in the cell. The match between observed and calculated images for braunite-II is also shown.

In Figure 7, a 5-module layer assemblage occurs together with a 42.6-Å (9-module) assemblage in braunite-II. The stacking sequence of the 5-module assemblage is one of two possibilities (nos. 9 and 10 in Table 3), but the one most compatible with braunite-II is number 9, the [BA′BA′A′] sequence, since part of it is a subset of the sequence of braunite-II. The postulated SiO_2 content of this assemblage is 4.0 wt%.

The 5-module layer assemblage also occurs in disordered braunite (Fig. 8). Again, the postulated image, with the [BA′BA′A′] stacking sequence, and the observed image are in qualitative agreement, whereas the postulated image from the other 5-module assemblage is not. The presence of additional A layers (those with whiter contrast in Fig. 8) complicates the image matching somewhat, but it shows that additional layer disorder exists among the braunite-II and 5-module assemblages.

Several examples of 8-module layer assemblages have been observed, mainly in braunite-II. In Figure 9, two 8-module assemblages with the probable stacking sequence of [BA′BA′A′BA′B] occur among the $[A'B]_4$ sequences of braunite-II. The SiO_2 content of all 8-module assemblages is postulated to be 5 wt%. This composition was confirmed qualitatively by AEM on 100-Å regions containing different 8-module assemblages. No differences in Si-peak intensities among these assemblages could be detected. The spot sizes were confirmed by visible beam damage of the specimen as a result of heating during analysis.

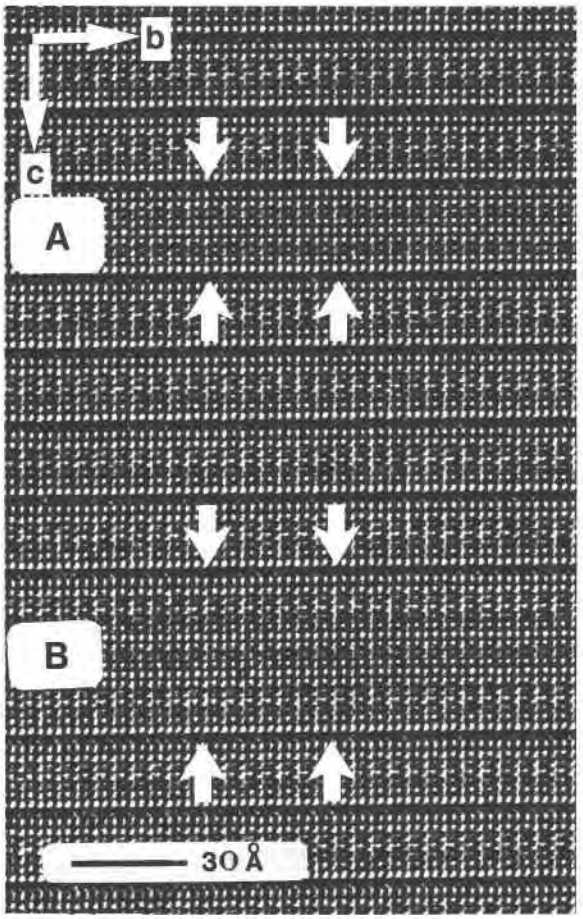

Fig. 7. A 5-module (23.6-Å) layer assemblage (A), together with a 42.6-Å assemblage (B) in braunite-II from Tachgagalt, Morocco. The arrows define the boundaries of each assemblage.

Differentiating among the various 37.8-Å polysomes is difficult because of the similarity of their calculated images. The minor differences among the calculated images are not generally evident in the experimental images, and it is therefore not always possible to determine which postulated 8-module assemblage is observed.

Assemblages with thicknesses greater than 37.8 Å occur in a number of samples. Most consist of several smaller assemblages (Fig. 10) and are associated with layer offsets. In order to save computing time and expense, image calculations of polysomes with thicknesses greater than 37.8 Å were not attempted. Moreover, most of these polysomes can be described as mixed-module sequences of smaller polysomes.

The SiO_2 contents of the polysomes (and layer assemblages) vary from zero to 10 wt% (Table 3). Depending on the relative abundances of the layer assemblages in a crystal, essentially continuous variations in SiO_2 contents are possible. In addition, ordered varieties of the postulated members in Table 3 may also exist. Several braunites whose compositions are given in the literature need to be re-examined in order to ascertain whether they are indeed ordered varieties of such polysomes. The relative

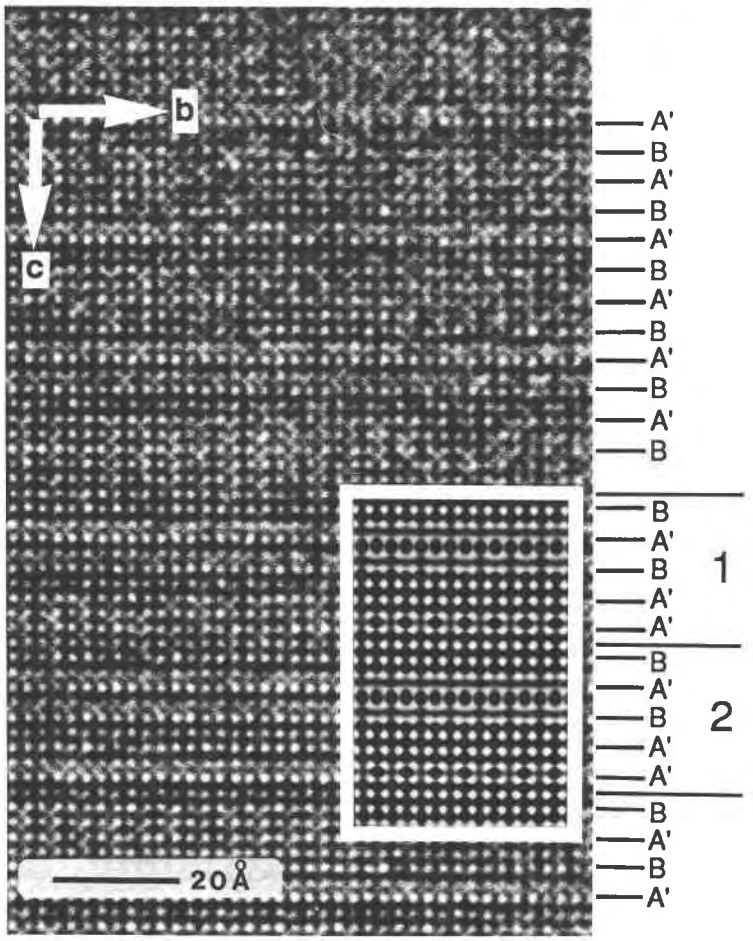

Fig. 8. A 5-module layer assemblage, [BA'BA'A'], in disordered braunite (from Dibiaghomo), with its superimposed calculated image derived from postulated atomic coordinates.

stabilities of the different polysomes are not currently known, but these will be calculated by use of energy-minimization procedures.

Microscopy of bixbyite-braunite-II intergrowths

The examination of disordered, nonstoichiometric braunite single crystals revealed another type of intergrowth that can explain variations in stoichiometry. Coherent intergrowths of braunite-II and bixbyite (Fig. 11) on a larger scale than shown above are common in these crystals. Intergrowths with variable amounts of the two components, one with zero and the other with 5% SiO_2, result in comparable variations in SiO_2 contents.

Figure 12 shows an interface between braunite-II and twinned bixbyite as well as compositional data. The optical diffraction patterns (note the relative intensities of the 020 vs. 002 spots of the two twin individuals) also suggest a noncubic symmetry for this bixbyite, which contains 13 wt% Fe_2O_3. This evidence is contrary to the findings of Geller (1971), who reported a cubic symmetry for bixbyite if the Fe_2O_3 content is greater than about 1 wt%. This qualitative observation would benefit from substantiation by X-ray structure analysis.

Another type of disorder also occurs in disordered braunite (Fig. 13). Layers of braunite-II are coherently and gradationally intergrown with bixbyite. Such intergrowths imply a mechanism different from the stacking operation perpendicular to the *c* axis of braunite-II. A dislocation mechanism is probably the most likely one.

Discussion and conclusions

The bixbyite-braunite mineral group is characterized by layer modules stacked in various ways to produce polysomes having different *c*-axis dimensions and compositions. Different layer assemblages are widespread and occur in even well-ordered "single crystals."

The structures of the polysomes or layer assemblages can be approximated closely by stacking of A layers in accordance with four stacking vectors. The interlayer cations occur in specific sites that depend on the coordination of the sites. These postulated structures were used as inputs for the calculation of simulated HRTEM images. The images were then used to elucidate the stacking sequences observed in experimental HRTEM images.

The materials examined show the following characteristics:

1. The bixbyite, which is extensively twinned, shows evidence of noncubic symmetry even with an Fe_2O_3 content of 13 wt%. This result is contrary to the findings of

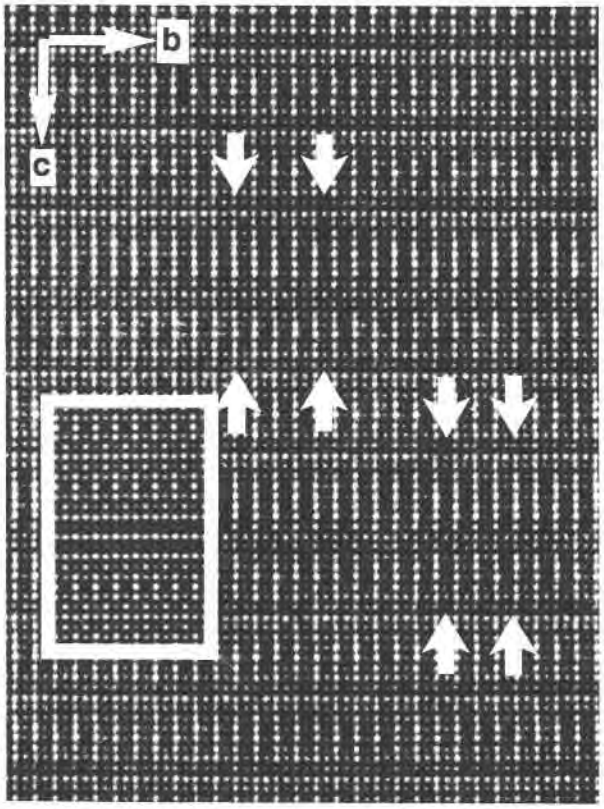

Geller (1971), who stated that bixbyite is cubic when it has an Fe_2O_3 content greater than 1 wt%.

2. Braunite-II contains layer assemblages of different thicknesses; the 5- and 8-module units are the most abundant. In addition, assemblages with thicknesses of 42.6, 47, and 52 Å have been observed. These can be described in terms of subunits of smaller thickness. The SiO_2 contents of these assemblages vary from 0 to 10 wt%. Depending on the relative amounts of the different assemblages in a crystal, any bulk composition between the above compositional limits is possible.

3. The disordered braunite crystals contain layer assemblages of different thicknesses, notably the 3-, 5-, and 8-module types, as well as intergrowths between these and bixbyite. The intergrowths occur on a scale ranging from single modules to layers several hundreds of angstrom units thick. Depending on the relative abundances of the two components, many compositional variations are possible.

4. Layers of braunite-II are coherently and gradationally intergrown with bixbyite in disordered braunite. A dislocation mechanism is proposed for this phenomenon.

←

Fig. 9. Two 8-module layer assemblages (from Middelplaats) having the same probable stacking sequences [BA′BA′A′BA′B] in a braunite-II host. The calculated image is shown for comparison. The arrows define the boundaries of each assemblage.

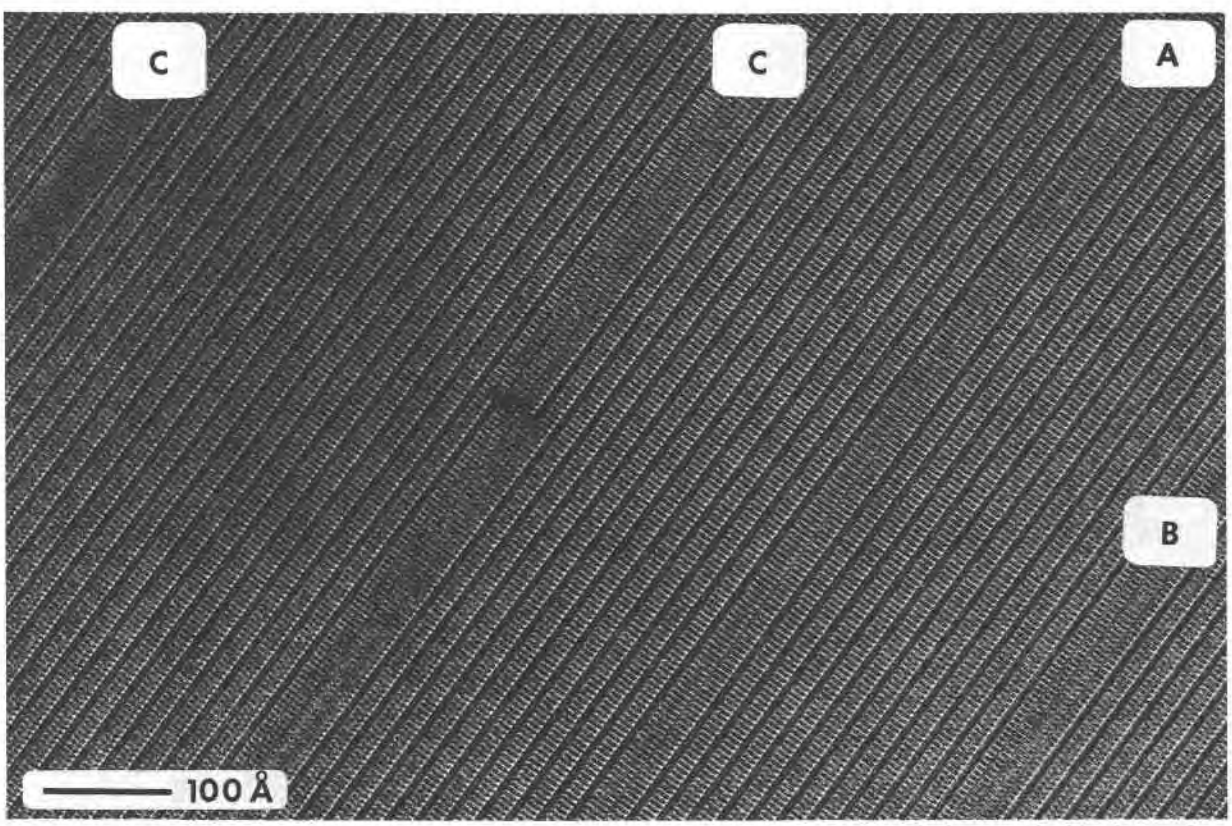

Fig. 10. Layer assemblages with thicknesses of 37.8 (A), 47 (B), and 52 Å (C) in braunite-II (from Middelplaats). The 52-Å unit is associated with a possible growth defect or dislocation.

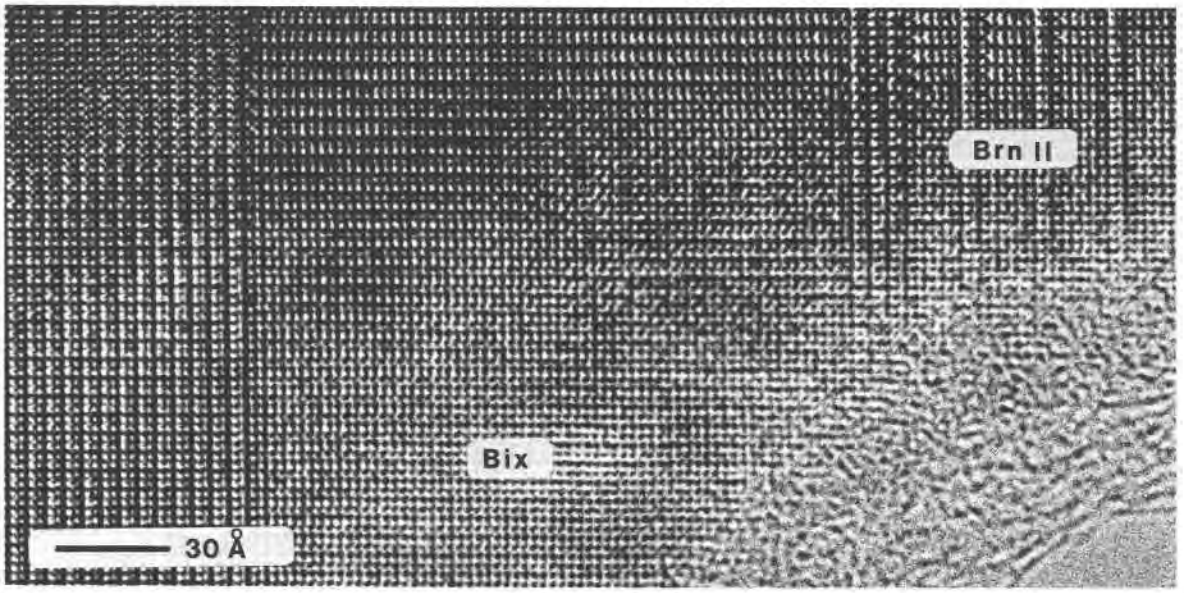

Fig. 11. Intergrowths of variable width between bixbyite (Bix) and braunite-II (Brn II) (from Dibiaghomo). Twinning in bixbyite can be seen in the left-hand side of the micrograph. The differences in contrast result from differences in orientation.

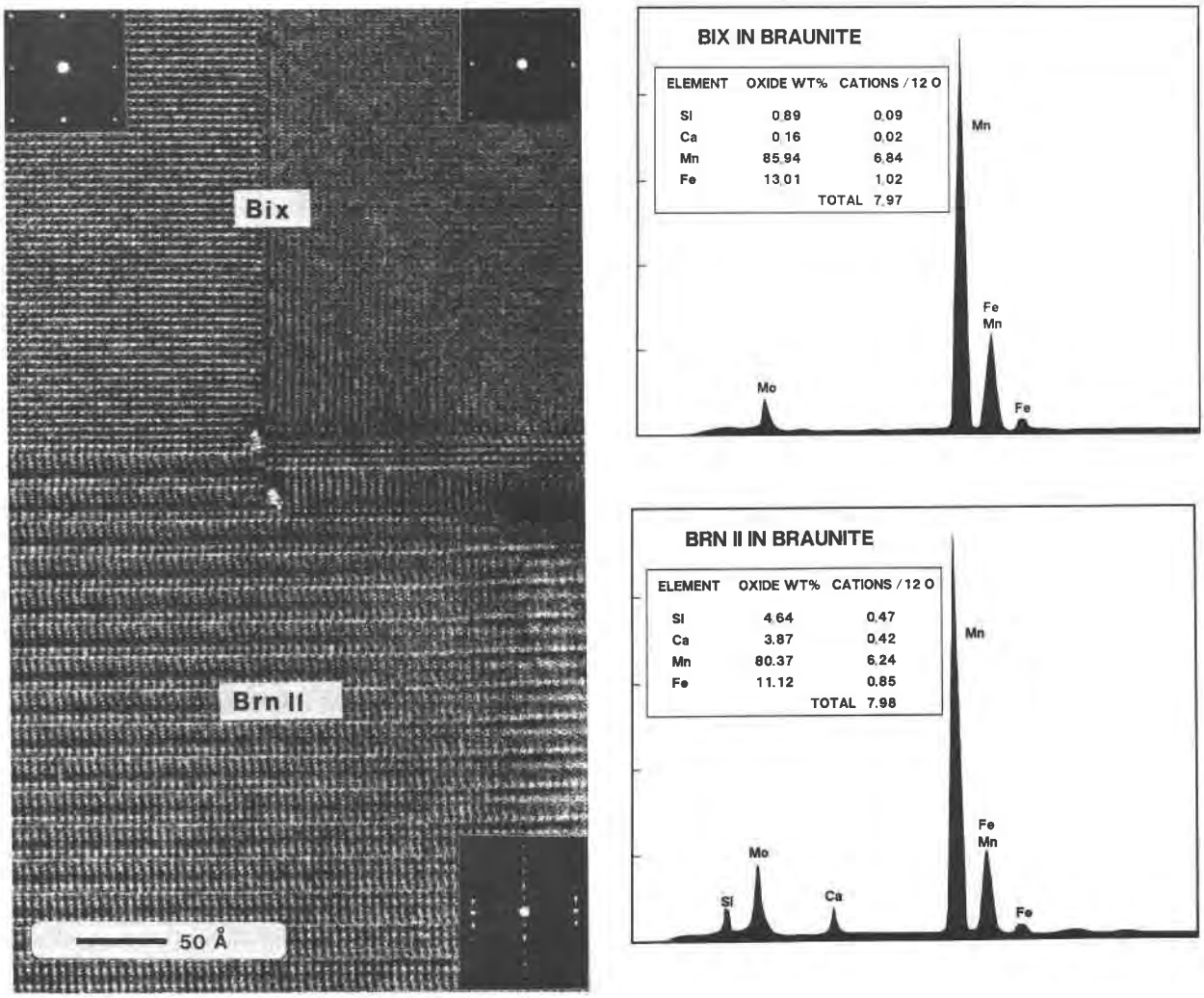

Fig. 12. Interface between braunite-II and twinned bixbyite (from Dibiaghomo). Optical diffraction patterns of the bixbyite twin individuals and braunite-II are shown as well as corresponding energy-dispersive analyses. The compositions are normalized on the basis of 12 oxygen atoms. The vertical axis in all three images and optical diffraction patterns corresponds to the *c* axis.

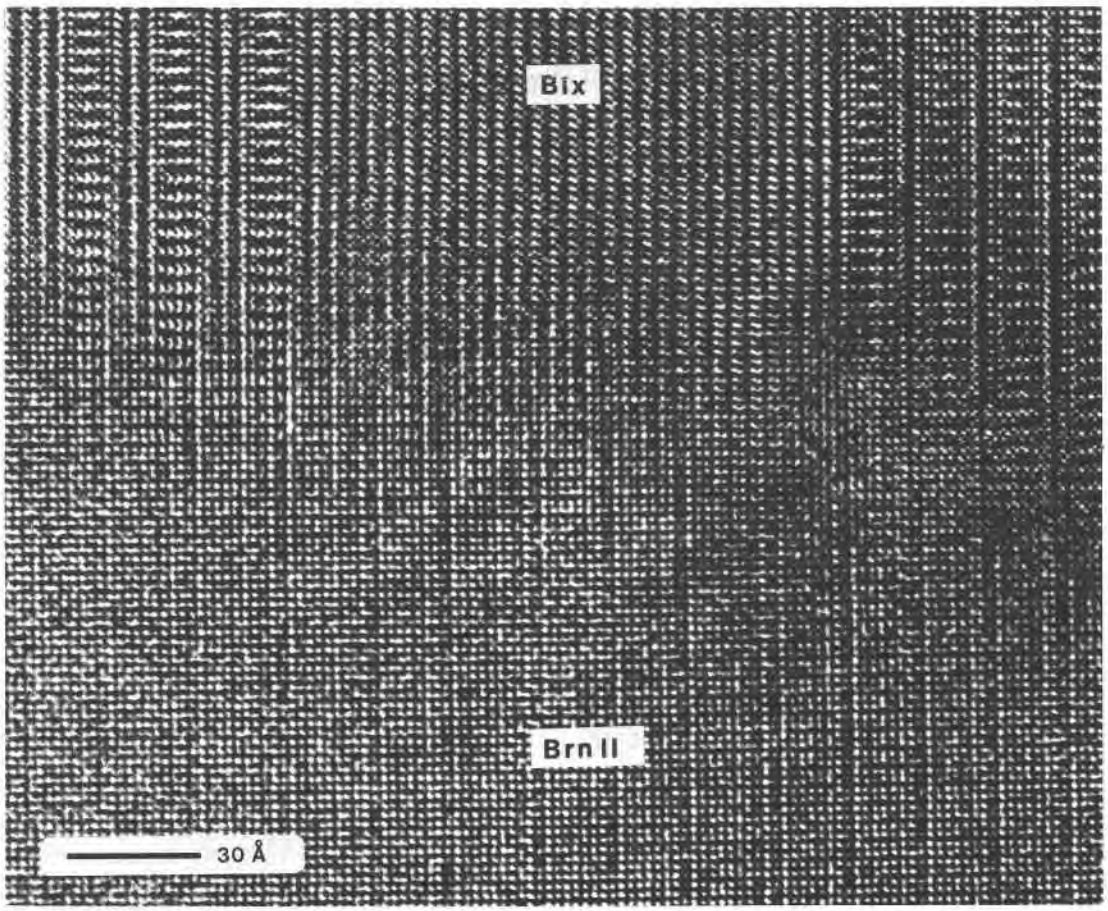

Fig. 13. Braunite-II layers gradationally and coherently in contact with bixbyite (from Dibiaghomo).

Several "braunites" whose compositions are reported in the literature need to be re-examined by single-crystal methods in order to determine whether ordered crystals of the observed or postulated polysomes exist. Specifically, braunite from Sitapar, India, with 8.52 wt% SiO_2 (Baudracco-Gritti, 1985), corresponds to the 7-module polysome with a theoretical SiO_2 content of 8.6 wt%. Also, a "braunite II" reported by Baudracco-Gritti (1985; analysis no. 4, p. 440), with an SiO_2 content of 6.6 wt%, corresponds closely either to the 3- or 6-module polysome with respect to SiO_2.

In light of the above findings, a few comments regarding nomenclature in this and related mineral groups are appropriate. Current practice, following the rules of the IMA Commission on New Minerals and Mineral Names, is that ordered crystals of members of polysomatic series be named as separate minerals when their X-ray characteristics are distinct. However, if a significant fraction of the hypothesized polysomes in this and related series were to be observed and then given unique names, the mineralogical literature could be swamped with new names. For example, in the case of the bixbyite-braunite mineral group, 21 names would potentially be necessary for polysomes containing up to a maximum of eight A-layer modules. For polysomes consisting of more modules, the number of possible members rises dramatically, creating the necessity of even more names.

A simplified version of the nomenclature proposed by Angel (1986) for the description of the various polysomes, similar to that of polytypes, is necessary for the systematic classification of various polysomatic series. In that case, the various braunite-related polysomes could be specified more precisely as, for example, braunite-[BA′B] for the 14.2-Å 3-module variety or, in the case of braunite-II, as braunite-$[BA']_4$. For such a convention to be useful, there needs to be a general knowledge and agreement regarding the modular units used to define the various polysomes. This is clearly an area for future work.

Acknowledgments

We thank John Barry, Carl Weiss, and John Wheatley of the Arizona State University (ASU) Facility for High Resolution Electron Microscopy for instruction and help with the microscopy and with assistance in the use of the image-simulation programs. Daniel Saucy provided valuable discussions and help with the programming of the polysome-stacking algorithm, and Jim Clark assisted with electron microprobe analysis. Dr. Celestine Baudracco and Professor Francois Permingeat of the Université Paul Sabatier, Toulouse, France, kindly provided samples of neltnerite and braunite-II. Helpful reviews were provided by Don Peacor and Paul B. Moore. This research was supported by the Earth Sciences Division of the National Science Foundation via grant EAR8708529. Electron microscopy was done at the ASU Facility for High Resolution Electron

Microscopy, which is supported by the NSF and ASU. The electron microprobe was purchased with the aid of NSF grant EAR8408163.

REFERENCES CITED

Angel, R.J. (1986) Polytypes and polytypism. Zeitschrift für Kristallographie, 176, 193–204.

Baudracco-Gritti, C. (1985) Substitution du manganese bivalent par du calcium dans les minéraux du groupe: Braunite, neltnerite, braunite II. Bulletin de Minéralogie, 108, 437–445.

Baudracco-Gritti, C., Caye, R., Permingeat, F., and Protas, J. (1982) La neltnerite. $CaMn_6SiO_{12}$, une nouvelle espèce minerale du groupe de la braunite. Bulletin de Minéralogie, 105, 161–165.

Buseck, P.R., and Veblen, D.R. (1988) Mineralogy. In P.R. Buseck, J.M. Cowley and L. Eyring, Eds., High-resolution transmission electron microscopy, p. 308–377. Oxford University Press, Oxford, England.

Damon, J.F., Permingeat, F., and Protas, J. (1966) Étude structurale du composé $CaMn_6SiO_{12}$. Comptes Rendus des Seances. Academie des Sciences (Paris), 262, 1671–1674.

de Villiers, J.P.R. (1975) The crystal structure of braunite with reference to its solid solution behaviour. American Mineralogist, 60, 1098–1104.

——— (1980) The crystal structure of braunite II and its relation to bixbyite and braunite. American Mineralogist, 65, 756–765.

Geller, S. (1971) Structures of alpha-Mn_2O_3, $(Mn_{0.983}Fe_{0.017})_2O_3$ and $(Mn_{0.37}Fe_{0.63})_2O_3$ and relation to magnetic ordering. Acta Crystallographica, 27, 821–828.

Ishizuka, K., and Uyeda, N. (1977) A new theoretical and practical approach to the multislice method. Acta Crystallographica, A33, 740–749.

Kleyenstüber, A.S.E. (1985) A regional mineralogical study of the manganese-bearing Voelwater subgroup in the northern Cape province, 328 p. Ph.D. thesis, Rand Afrikaans University, South Africa.

Kohn, J.A., and Eckart, D.W. (1965) Stacking relations in the hexagonal barium ferrites and a new series of mixed-layer structures. Zeitschrift für Kristallographie, 119, 454–464.

Magneli, A. (1953) Structures of the ReO_3 type with recurrent dislocations of atoms: "Homologous series" of molybdenum and tungsten oxides. Acta Crystallographica, 6, 495–500.

Moore, P.B., and Araki, T. (1976) Braunite: Its structure and relationship to bixbyite, and some insights on the genealogy of fluorite derivative structures. American Mineralogist, 61, 1226–1240.

Thompson, J.B. (1978) Biopyriboles and polysomatic series. American Mineralogist, 63, 239–249.

Veblen, D.R., and Buseck, P.R. (1979) Chain-width order and disorder in biopyriboles. American Mineralogist, 64, 687–700.

MANUSCRIPT RECEIVED JANUARY 17, 1989
MANUSCRIPT ACCEPTED JULY 26, 1989